Towards Reliable Simulations of Core-Collapse Supernovae

Paris ,IHP, July 08

Eli Livne (HUJI)

Collaboration : "Tucson AZ group" –

A. Burrows, L. Dessart, C. Ott, J. Murphy

Content

- 1. Introduction
- 2. Description of V2D
- 3. Some examples and results
- 4. Lessons
- 5. Conclusions and future work

1. Introduction

Progenitors of Type II Sne

Massive stars of 10-40 solar masses evolve to form partially degenerate iron cores.

The core becomes unstable to collapse as its mass approaches Chandrasekhar mass. Due to electron capture and iron dissociation to alpha particles the effective \Gamma drops below 4/3

Schematic Post-Bounce Configuration
H.-Th. Janka and W. Keil 1997

The shock stalls and becomes a standing accretion shock. The 1D structure is (from inside out) : core at nuclear densities (PNS), cooling region, heating region, accretion shock, infalling matter.
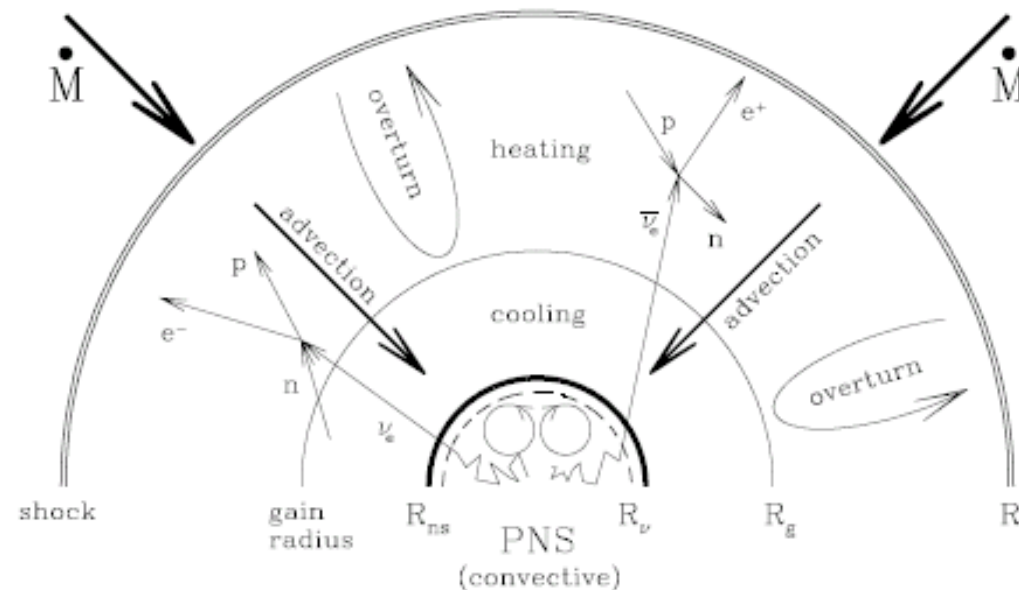One of the largest graveyards for theories !!

Figure 1.   Sketch of the post-collapse stellar core during the neutrino heating and shock revival phase. At the center, the neutrino emitting

Explosions as Critical Phenomena
Burrows & Goshy 1993
steady state configurations

BURROWS & GHOSY   Vol. 416

Critical Curve
T_ν = 4.5 MeV

SUPERNOVA

MODEL TRAJECTORY

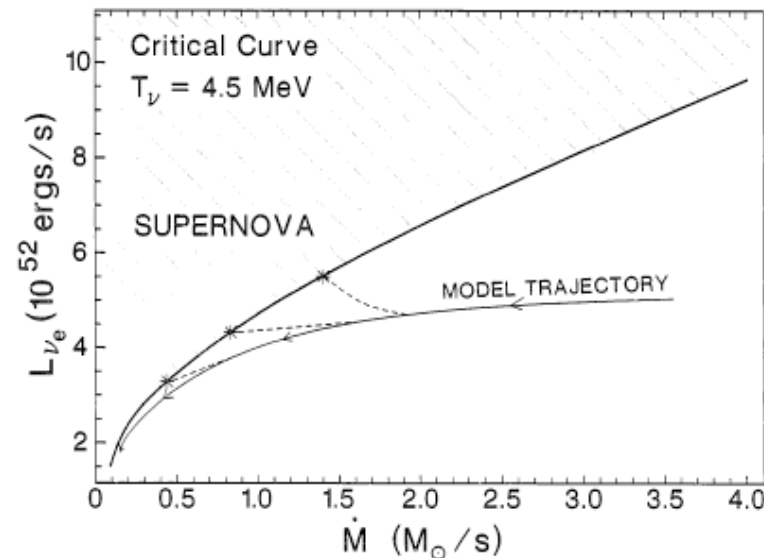L_{ν_e} (10^{52} ergs/s)

$\dot{M}$ ($M_\odot$/s)

FIG. 1.—Depicted in L_{ν_e} (in units of 10^{52} ergs s^{-1}) vs. $\dot{M}$ (in units of $M_\odot$ s^{-1}) space are the critical curve (*heavy solid line*) of Table 1 (and approximately of eqn. [6]) and a representative model trajectory (*solid line*) of "unsuccessful" core evolution, similar to that found in Bruenn 1992. If the evolution line of a real core crosses the critical curve into the hatched region, a neutrino-driven supernova should begin.

Multi-dimensional effects absent in the 1D picture

- Convection inside the PNS and below the shock
- SASI - Instability of the shock
- Rotation
- Magnetic fields and bi-polar jets

interactions between the above

And : Observations of remnants revealing non-spherical structures (CAS A) suggest non-spherical explosion mechanisms.

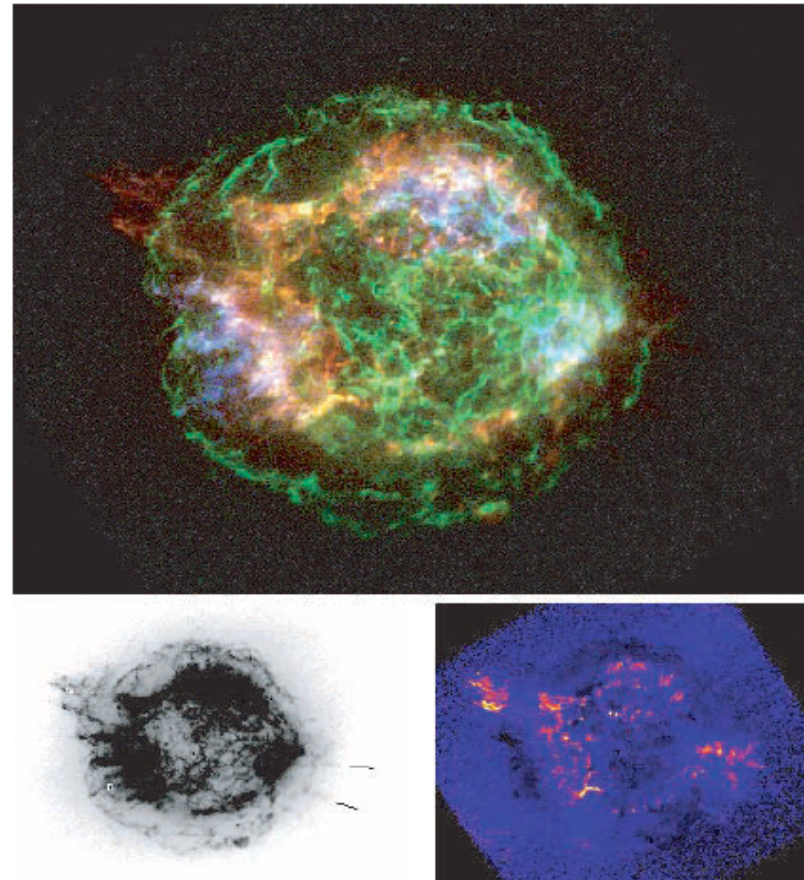# Core-Collapse SN remnants show strong non-spherical structures and bi-polar jets (Cas A)

FIG. 1.—*Top:* Three-color image of Cas A with red = Si Heα (1.78–2.0 keV), blue = Fe K (6.52–6.95 keV), and green = 4.2–6.4 keV continuum. The remnant is roughly 5' across. *Bottom left:* Overexposed broadband image showing faint features. The spectral regions are indicated (*top left box:* northeast jet; *bottom left box:* Fe-rich region; lines at bottom right point to two southwest jet filaments). Smearing associated with CCD readout causes the low surface brightness artifacts outside the remnant to the southeast and northwest. *Bottom right:* On the same scale, the ratio image of the Si Heα (1.78–2.0 keV) and 1.3–1.6 keV (Mg Heα, Fe L), without subtraction of the continuum contribution. The image highlights the jet and counterjet traced by Si emission, although features at the lowest intensity levels are uncertain.

Why multi-D simulations of c-c are so exceptionally difficult ?

- <u>Time scales</u> – many dynamical times within 1 sec

  1 million time steps of roughly 1 microsecond are needed

  for 1 second (the flow within the shock radius is very subsonic, dominated by rotational component).

- <u>Resolution</u> – most of the mass is enclosed after bounce

  in a small region around the PNS, covered by a small

  number of zones !!

- <u>Accuracy</u> - The balancing forces are huge and their net

  difference is responsible for the action. Equivalently – the explosion energy is a small fraction of the internal or gravitational energy.

  For example – a numerical error of $10^{-7} * 10^{53}$ erg, per time step, will accumulate an error of 10^{51} erg in 100,000 time steps.

- <u>Complicated neutrino radiation field, stiffly coupled to matter</u>

2.   2D Simulations using VULCAN/2D

Components of the code : Newtonian dynamics in cylindrical symmetry

- Arbitrary Lagrangian-Eulerian hydro (ALE); remapping, and no singularity at the center

- Several gravity solvers

- 2D multi-group (parallelized) neutrino diffusion (MGFLD), or angle dependent neutrino transport

- Axial rotation with exact conservation of angular momentum

- Magnetic Fields

- Several equations of state/neutrino cross-sections

Livne 1993, Burrows et al. (2004), Ap.J., 609, 277; Walder et al. (2005), Ap.J., 626, 317; Ott et al. (2004) Ap.J., 600, 834; Burrows et al. (2005), Ott et al. (2005)

The inner grid - removes the singularity of polar grids and enables free streaming along the axis
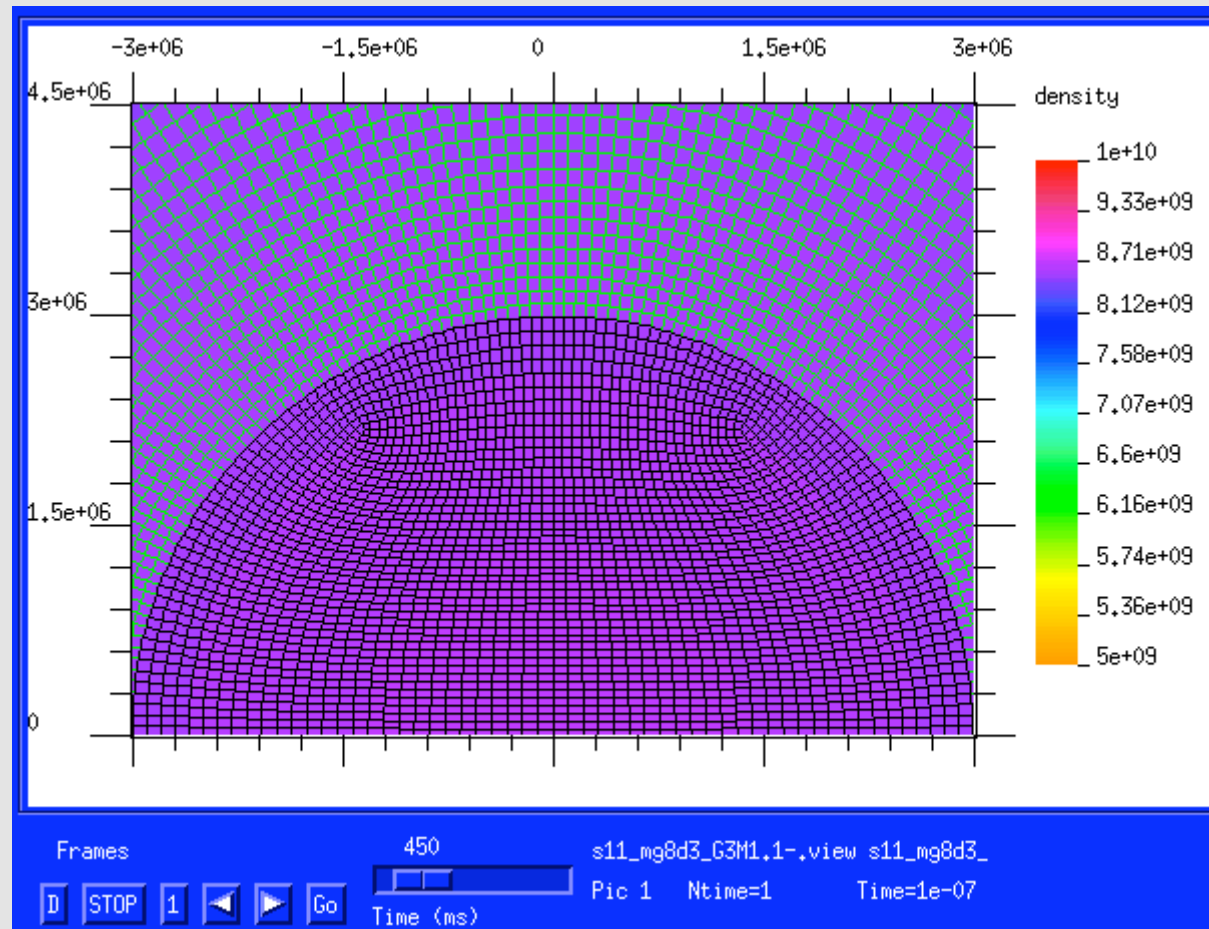
Gravity Solvers

- Legendre polynomials
- Finite Element Grid Solver
- Finite Difference Grid Solver

Conserving linear momentum under gravity :

$$\rho \frac{D\mathbf{v}}{Dt} = -\nabla p + \rho \nabla \Phi$$

The gravity term in this momentum equation has no conservative form - direct finite differencing of this term should and will violate conservation of linear momentum

conservative forms using gravitational stress tensor (Shu, Hydrodynamics , p 47)

$$\mathbf{f_g} = -\rho \nabla \phi = \frac{1}{4\pi G} \Delta \phi \nabla \phi$$

$$\mathbf{f_g} = \mathbf{div(S)}$$

$$\mathbf{g} = \nabla \phi \text{ (F.H.Shu p.47) :}$$

$$\mathbf{S_{ij}} = \frac{1}{4\pi G}(g_i g_j - \frac{1}{2} \mid \mathbf{g} \mid^2 \delta_{\mathbf{ij}})$$

$$f_z = \frac{1}{4\pi G}\{\frac{1}{r}\frac{\partial(rg_r g_z)}{\partial r} + \frac{1}{2}\frac{\partial(g_z^2 - g_r^2)}{\partial z}\}$$

$$f_r = \frac{1}{4\pi G}\{\frac{1}{2r}\frac{\partial[r(g_r^2 - g_z^2)]}{\partial r} + \frac{\partial(g_r g_z)}{\partial z} + \frac{1}{2r}(g_r^2 + g_z^2)\}$$

Neutrino Radiation Hydrodynamics

- The Neutrino-Driven Mechanism (Wilson 1985) :

  The neutrino radiation field with luminosity of the order of 10^{53} erg/sec may deposit the required explosion energy in the mantle (10^{51} erg= 1B) over a period of a few seconds.

- The coupling of neutrinos to matter occurs via the processes : emission, absorption and scattering. Cross sections for those are complicated functions of density, temperature, composition and neutrino specie and energy (will not be discussed here)

- But, the cross sections are very small and therefore the problem is horribly complicated

Neutrino Radiation Techniques (Livne etal. ApJ,609,2004):

Lab-Frame approximations for neutrino radiation field :

- Flux limited multi group diffusion - FLMGD
  (with 8-16 energy groups and 3 neutrino species)
  parallelized by groups and species

- Angle dependent multi group TRANSPORT
  (with 8-16 energy groups and 3 neutrino species)
  parallelized by groups and species
  roughly 50-100 directions for each energy bin   !!
  Currently do not include velocity terms

Multi angle S_n transport

In 2D axisymmetric geometry, the transport equation becomes

$$\frac{1}{c}\frac{\partial\Psi}{\partial t} + \mu\frac{\partial\Psi}{\partial r} + \eta\frac{\partial\Psi}{\partial z} - \xi\frac{\partial\Psi}{r\partial\phi} + \sigma\Psi = S \qquad (19)$$

or in conservative form :

$$\frac{1}{c}\frac{\partial\Psi}{\partial t} + \frac{1}{r}\frac{\partial(r\mu\Psi)}{\partial r} + \eta\frac{\partial\Psi}{\partial z} - \frac{1}{r}\frac{\partial(\xi\Psi)}{\partial\phi} + \sigma\Psi = S. \qquad (20)$$

Here, the directional cosines are just the projections of the unit vector $\mathbf{\Omega}$ (in the velocity direction) on the Cartesian axes (Figure 3):

$$\eta = \cos(\theta)$$

$$\mu = \sin(\theta)\cos(\phi)$$

$$\xi = \sin(\theta)\sin(\phi),$$
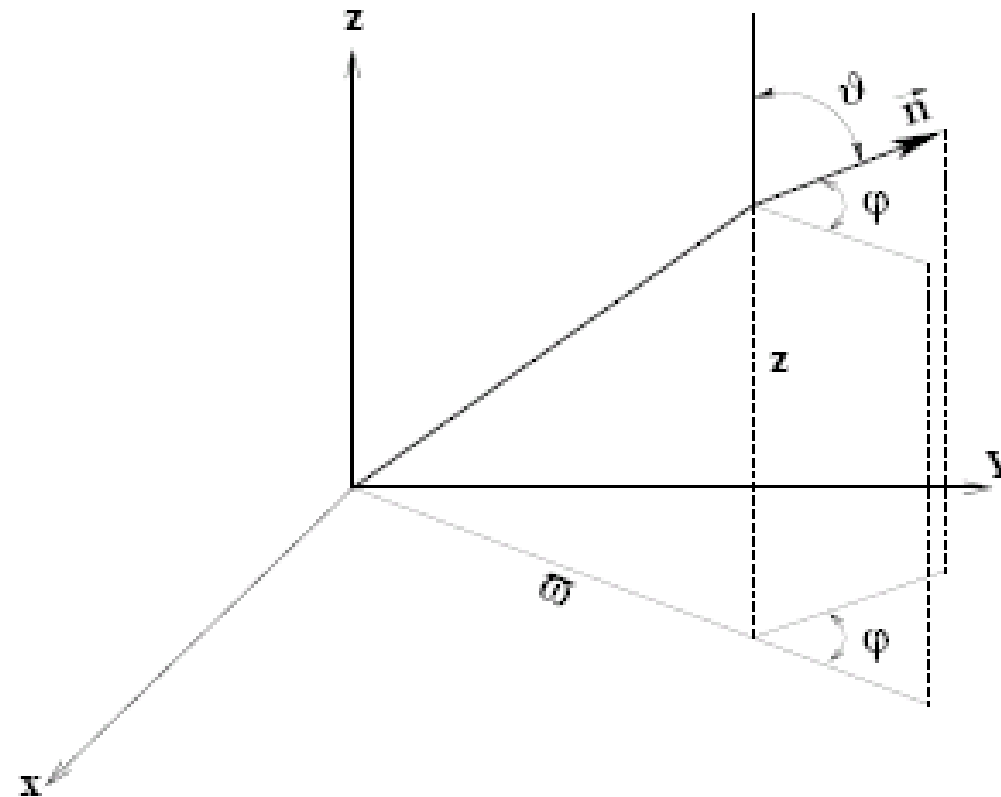
Angles of the transport scheme

FIG. 1.— Coordinates used in the axisymmetric S_n transport scheme implemented in VULCAN/2D. The radiation direction vector $\bar{n}$ is defined in terms of ϑ and φ. ϑ is the angle with respect to the coordinate-grid z-axis at all spatial positions (z, ϖ). At each (z, ϖ), the local momentum-space unit sphere is covered by n zones in ϑ and at each ϑ location by a number $m(\vartheta)$ of φ-zones, so that the each zone in (ϑ, φ) covers roughly the same solid angle.
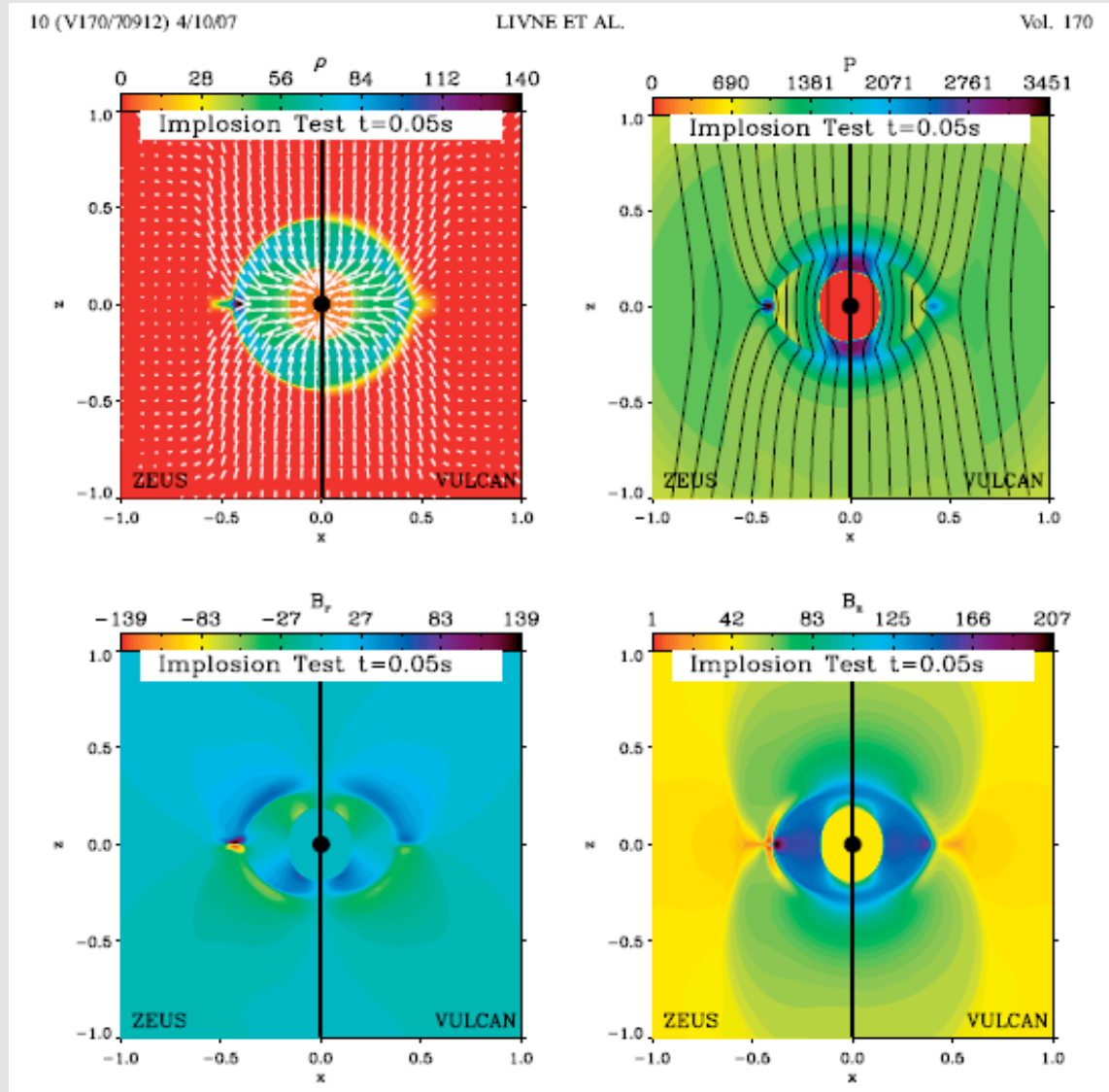
The Hydro-Magnetic Solver (Livne etal,ApJS,170,187,2007)

- Adapted to non-structured grids, and ALE
- Explicit
- Exactly conserves div(**B**)=0
- Second order accurate
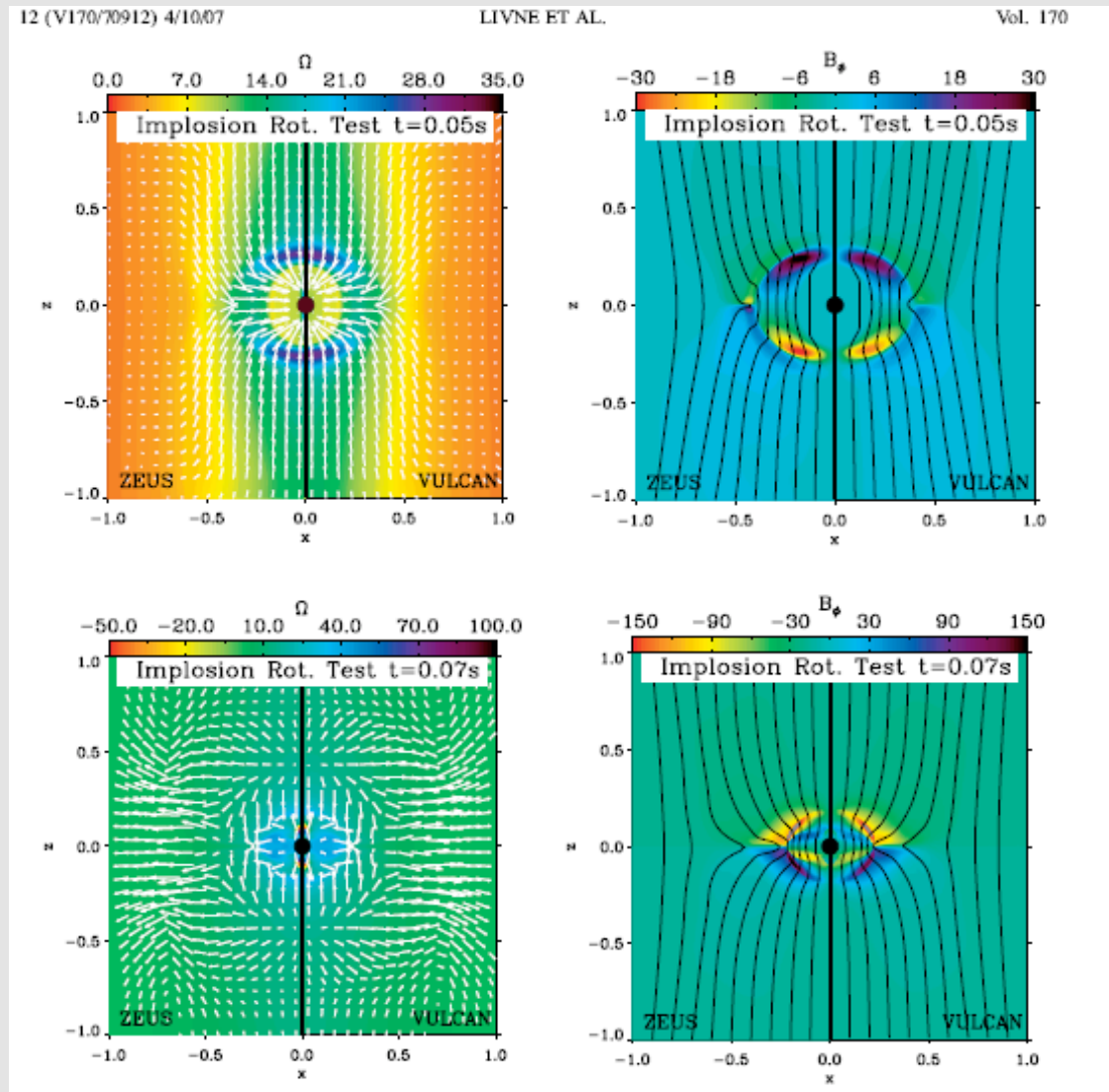
Brio-Wu 1D test problem
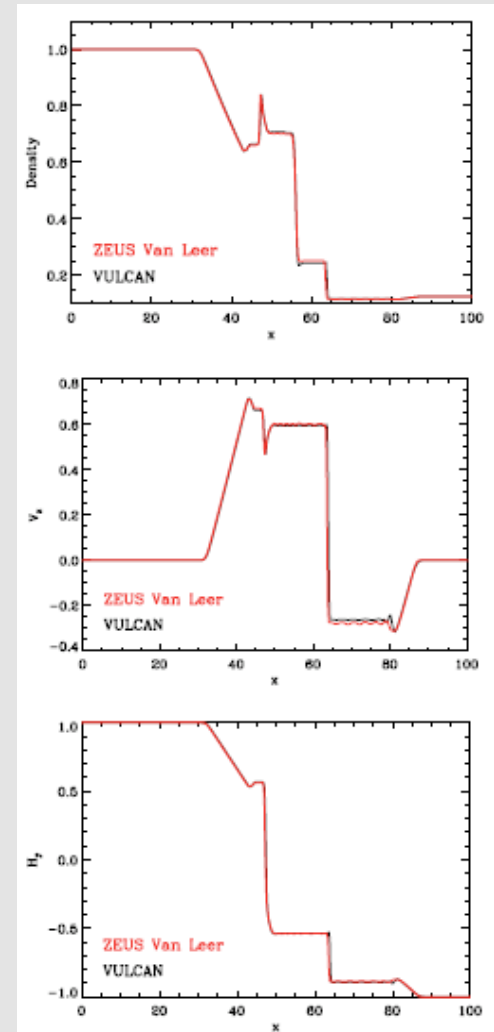
Testing the code against Zeus/2D

continue

3. Some examples and results

Numerical parameters

N_rad=200, N_theta=120

3 Neutrino species (nu_e, nu_p, others)

8 – 16 neutrino energy groups

Typical post-bounce time step - 1 microsecond

A few weeks of CPU time on a cluster of 12 processors.

With transport – roughly 50 angles for each energy bin for
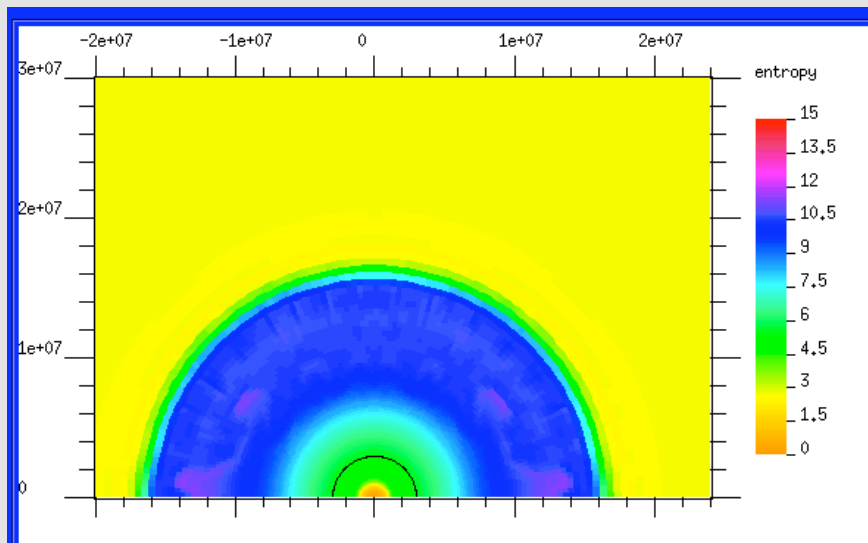minimal angular resolution

Evolution of Convection

Convection above the PNS alters the 1D picture drastically.

It evolves within about 100 ms after bounce by neutrino heating below the shock.

The convective speed reaches roughly 10^9 cm/sec and the convective currents may provide another efficient energy transport.

Herant etal. (1994) used 2D SPH simulations, with very crude neutrino physics, to claim that explosion occurs due to convection, which carries enough heat from the inner regions to the shock region.
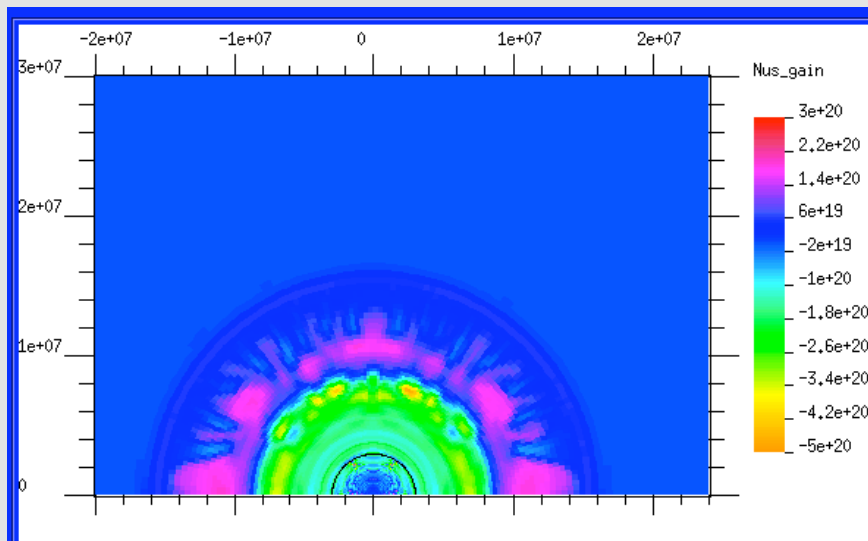
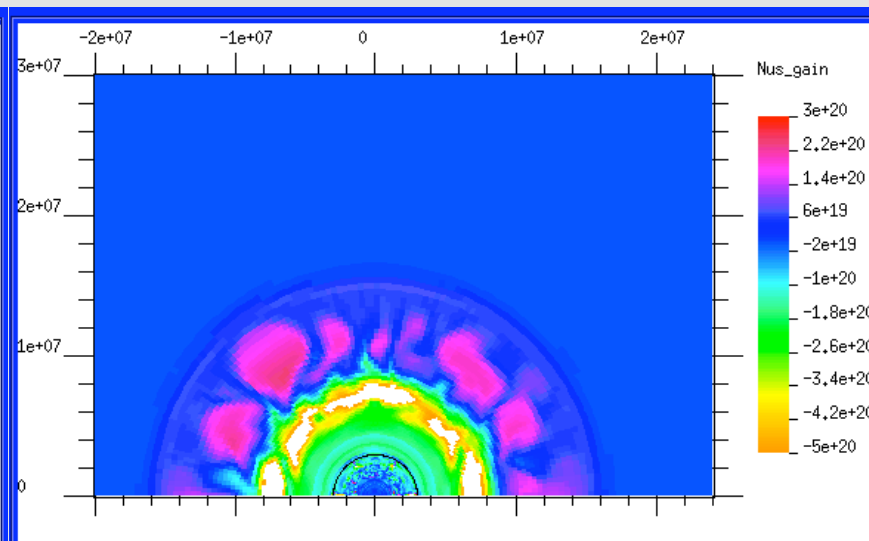Later – this was disproved by more detailed multi-group neutrino physics (Rammp & Janka 2202, Buras etal. 2003)

Top-left panel:

entropy

15
13.5
12
10.5
9
7.5
6
4.5
3
1.5
0

Frames

D STOP 1 ◄ ► Go

450

Time (ms)

s11_mg8d3_G3M1.87382-.view s11_mg8d3_

Pic 1   Ntime=87382   Time=0.325

Top-right panel:

entropy

15
13.5
12
10.5
9
7.5
6
4.5
3
1.5
0

Frames

D STOP 1 ◄ ► Go

450

Time (ms)

s11_mg8d3_G3M1.104856-.view s11_mg8d3_

Pic 2   Ntime=104856   Time=0.35

Bottom-left panel:

Nus_gain

3e+20
2.2e+20
1.4e+20
6e+19
-2e+19
-1e+20
-1.8e+20
-2.6e+20
-3.4e+20
-4.2e+20
-5e+20

Frames

D STOP 1 ◄ ► Go

450

Time (ms)

s11_mg8d3_G3M1.87382-.view s11_mg8d3_

Pic 1   Ntime=87382   Time=0.325

Bottom-right panel:

Nus_gain

3e+20
2.2e+20
1.4e+20
6e+19
-2e+19
-1e+20
-1.8e+20
-2.6e+20
-3.4e+20
-4.2e+20
-5e+20

Frames

D STOP 1 ◄ ► Go

450
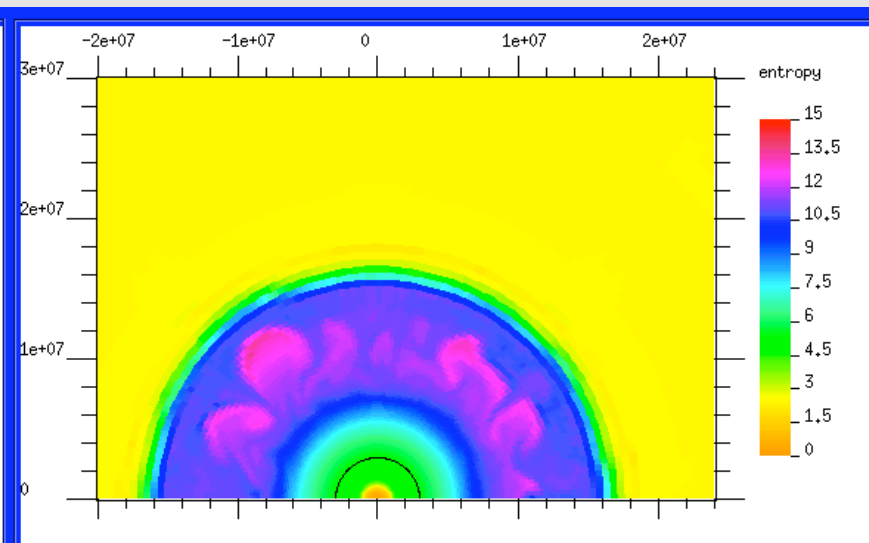
Time (ms)

s11_mg8d3_G3M1.104856-.view s11_mg8d3_

Pic 2   Ntime=104856   Time=0.35

Evolution governed by SASI

- t=30 ms : formation of a spherical accretion shock
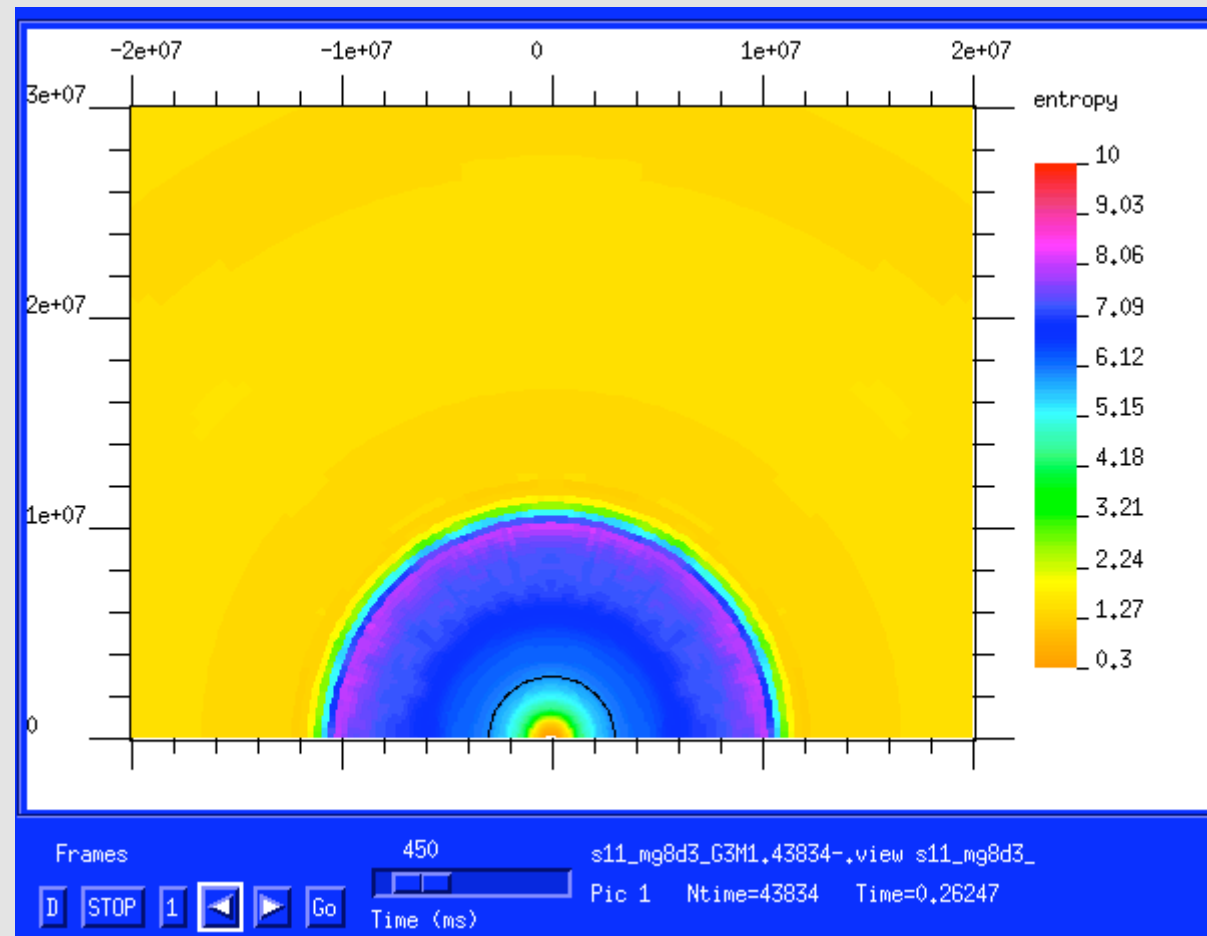
t=120 ms : convection destroys symmetry
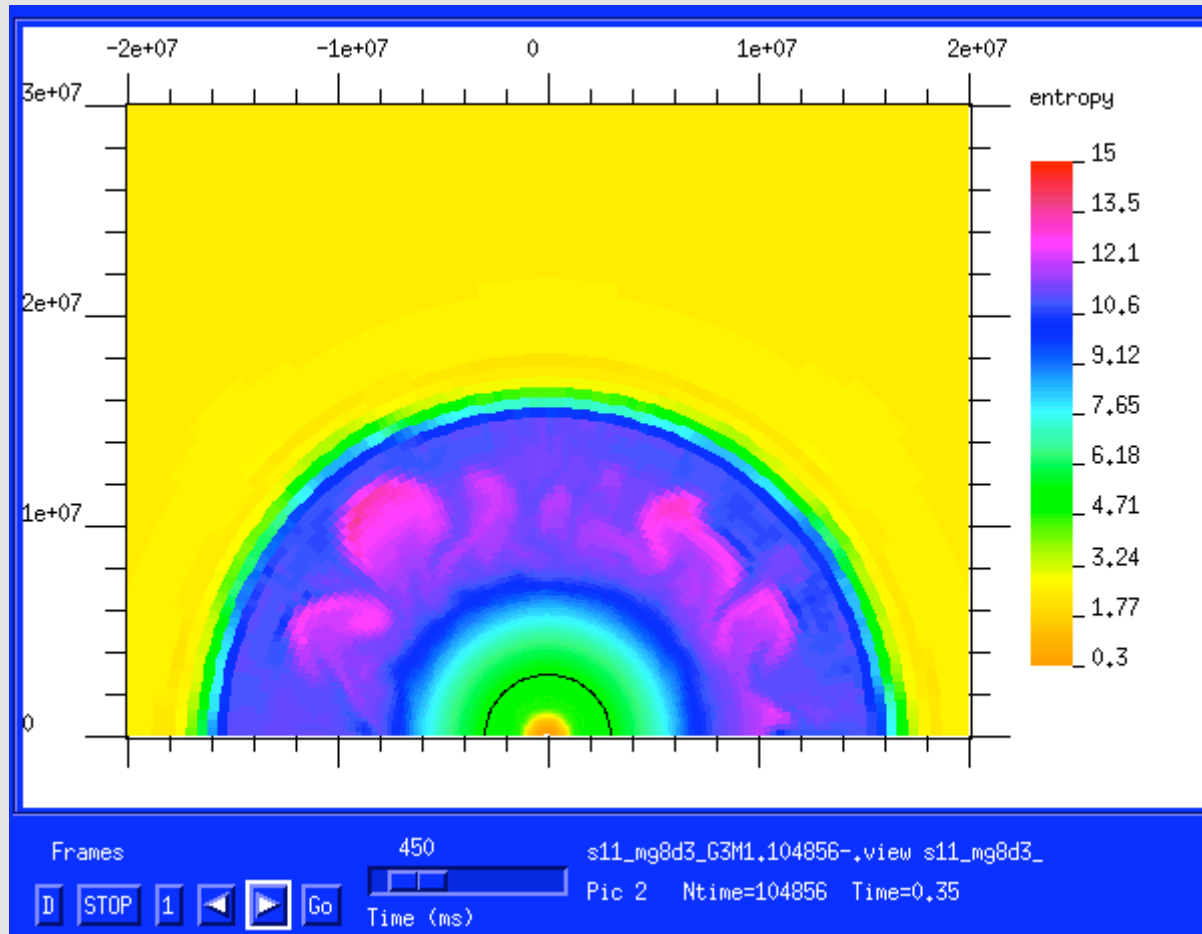
t=190 ms   : growing L1 modes oscillations develop (onset of SASI)

t=220 ms : extra heating by multiple shocks between up-streams and the infall drives the instability further

t=270 ms , SASI in the very non-linear phase

t=370 ms,   further expansion and increase of entropy

Similar other works
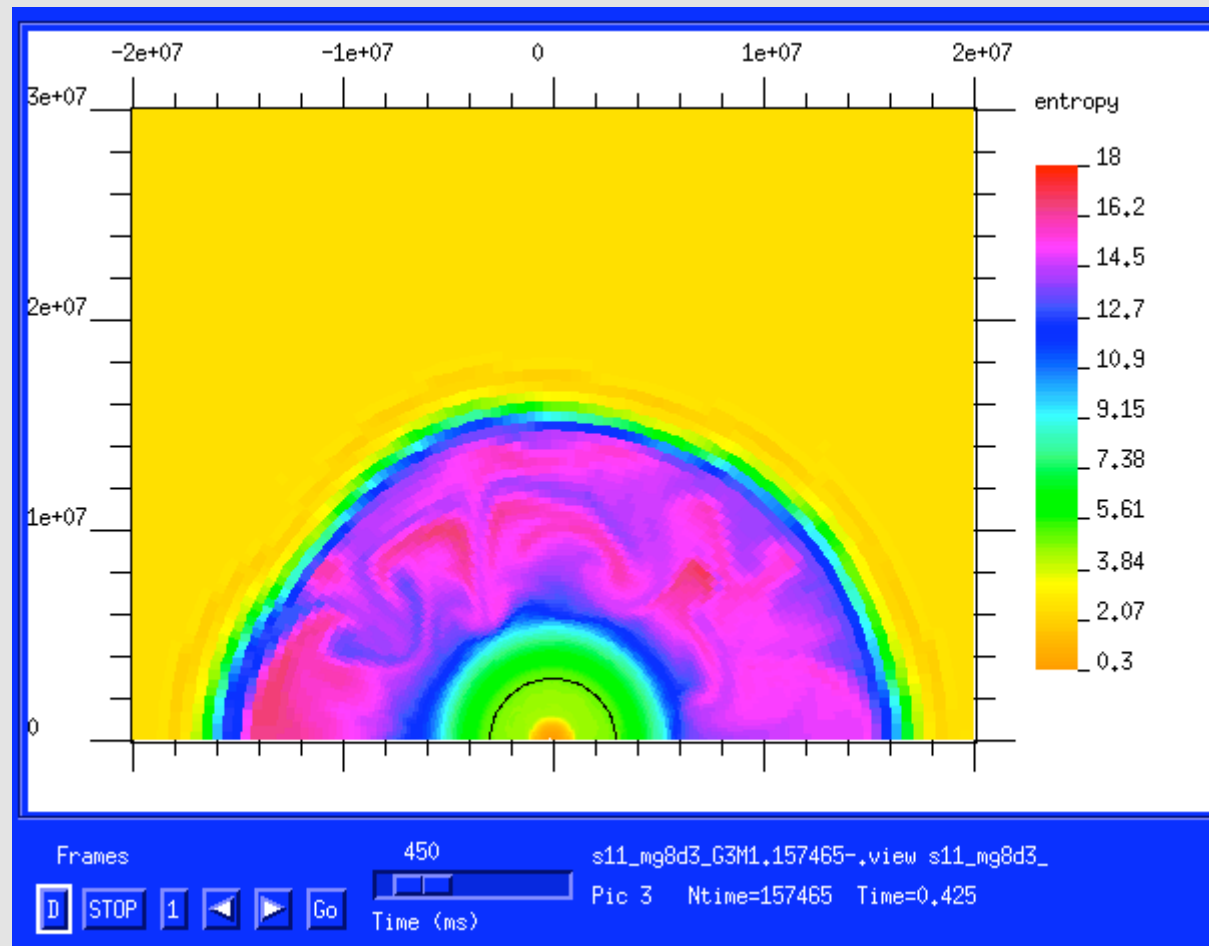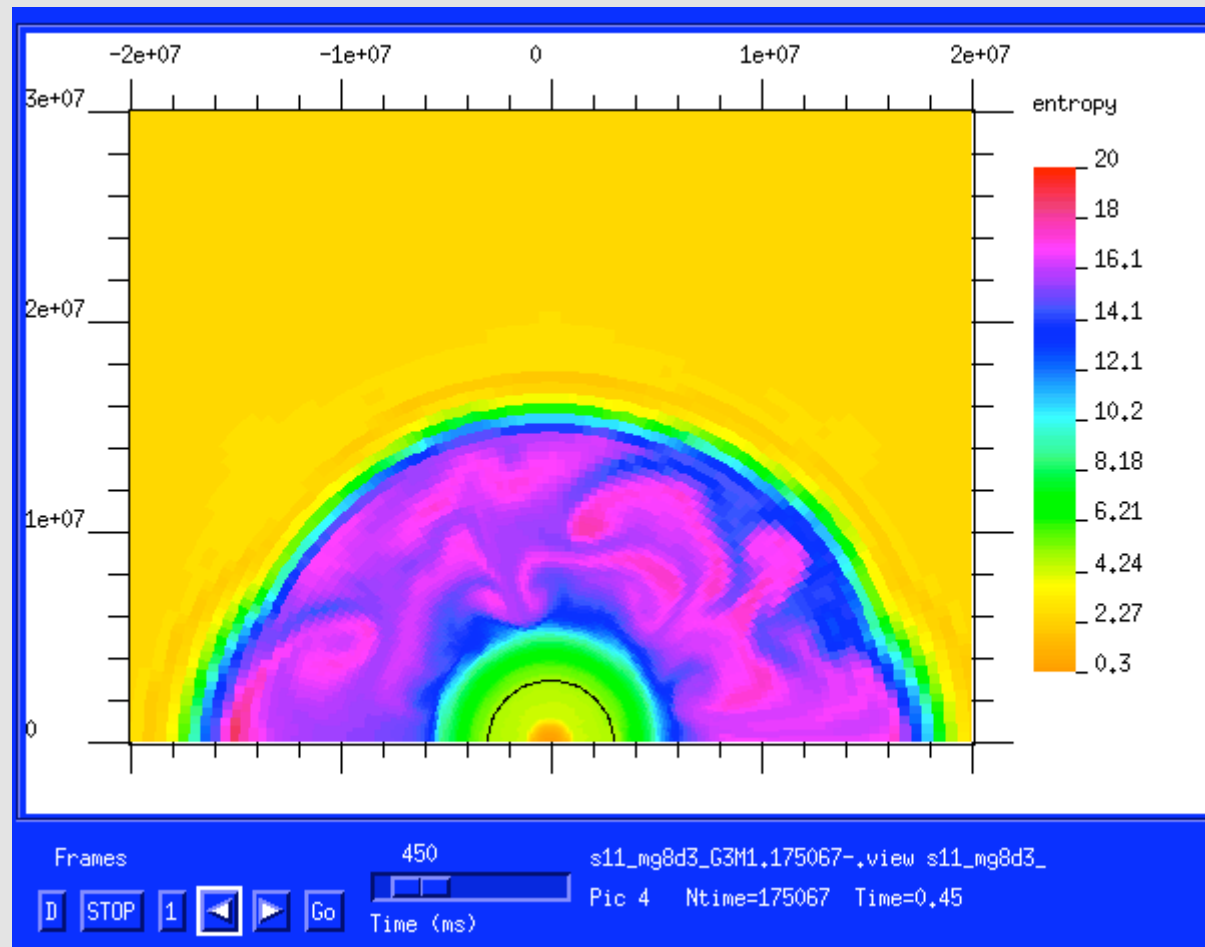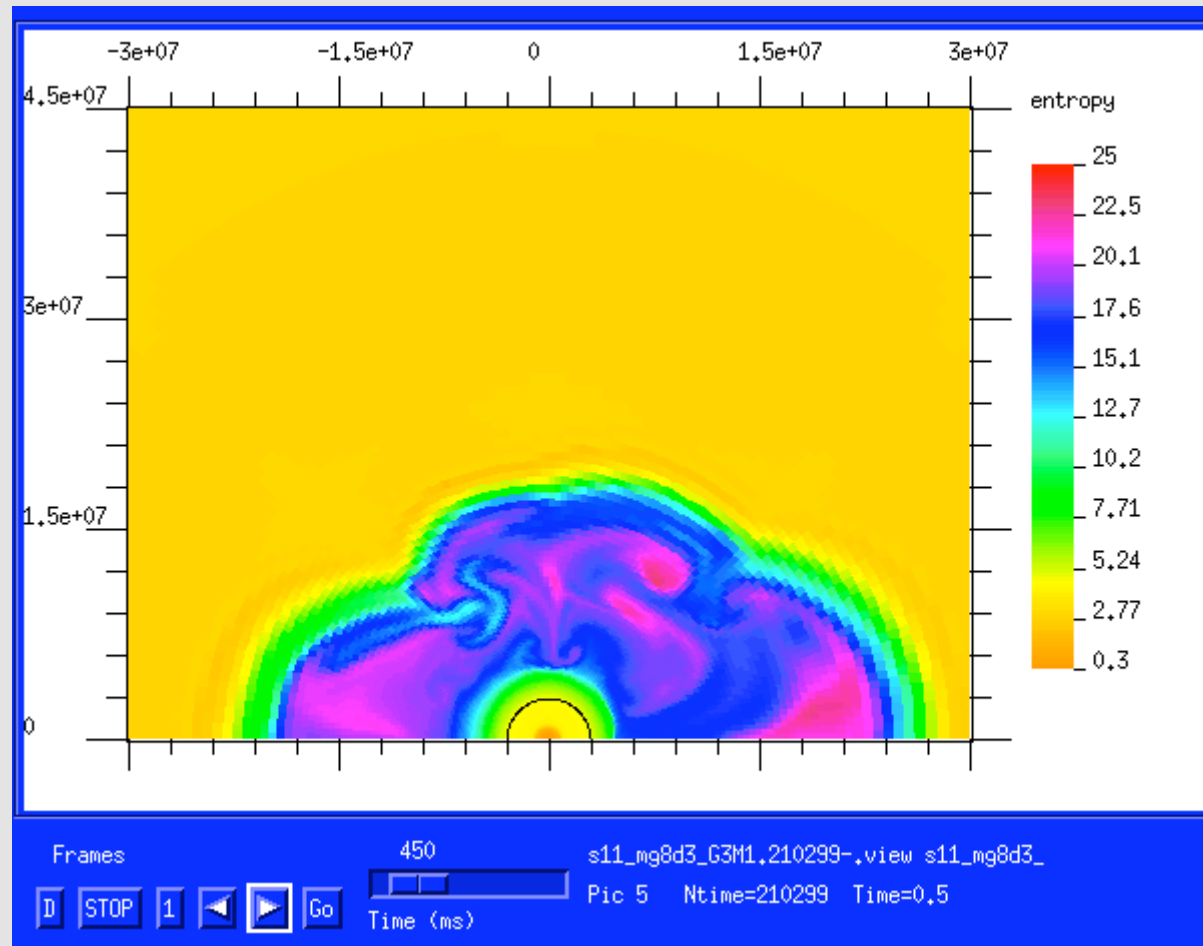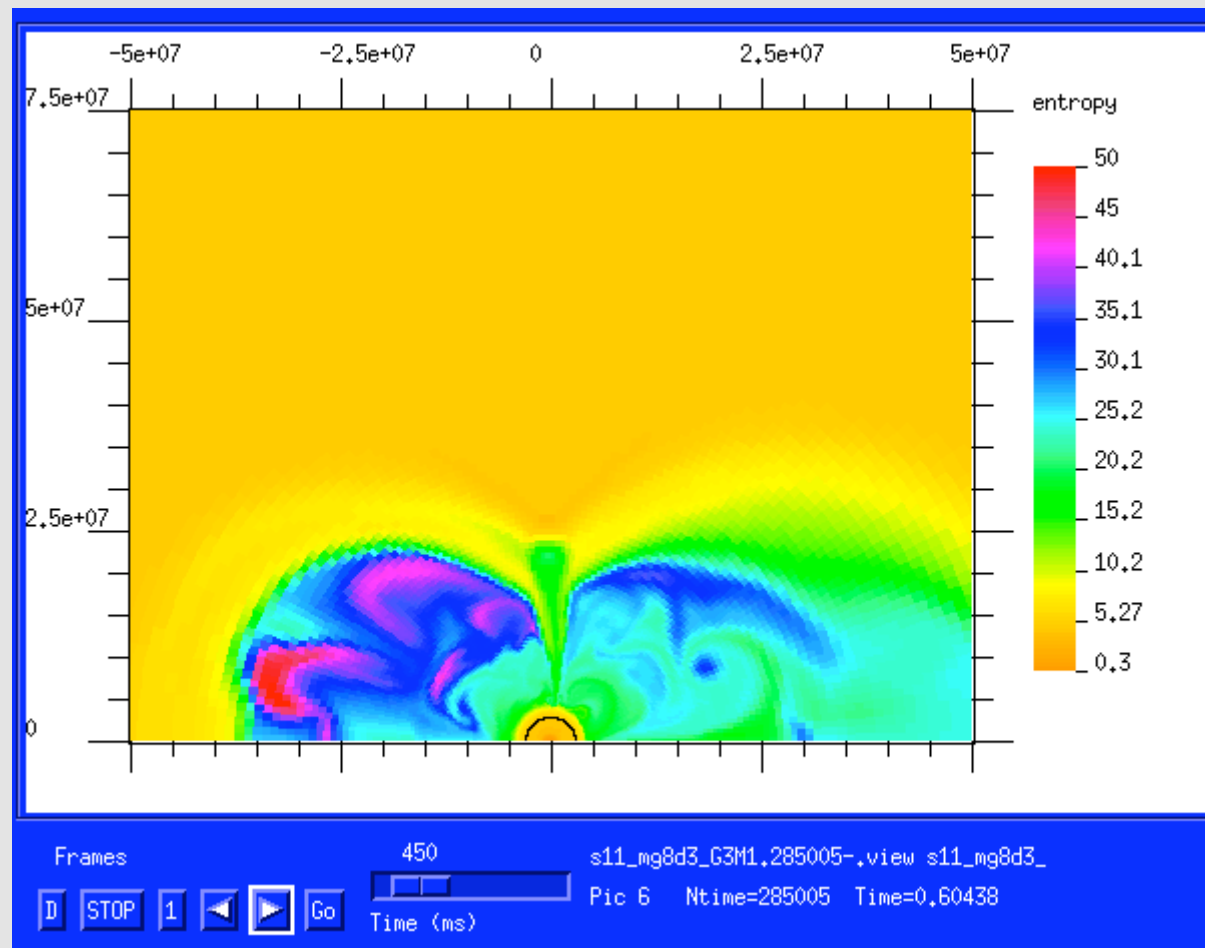
Marek & Janka 2007 (15 M_o 2D)

FIG. 3.— Four snapshots from the post-bounce evolution of Model M15LS-rot. The color coding represents the entropy of the stellar gas. The shock is visible as deformed sharp discontinuity between low-entropy, infalling matter in the upstream region and high-entropy, boiling matter behind the shock. The upper left plot shows the entropy distribution at $t = 119$ ms after bounce, about 40 ms after the postshock convection has reached the nonlinear regime. The upper right and lower left plots ($t = 454$ ms and $t = 524$ ms after bounce) demonstrate the presence of a very strong bipolar oscillation due to the SASI, and the lower right plot ($t = 610$ ms p.b.) displays the onset of a rapid outward expansion, most likely leading to an explosion, of the largely aspherical shock with a dominant $l = 1$ deformation mode. Note that the contracting nascent neutron star exhibits a growing prolate deformation because of the rotation considered in this simulation. The thin white line marks the direction-dependent location of the gain radius.

no explosion

(low L_nus)

explosion

(high L_nus)

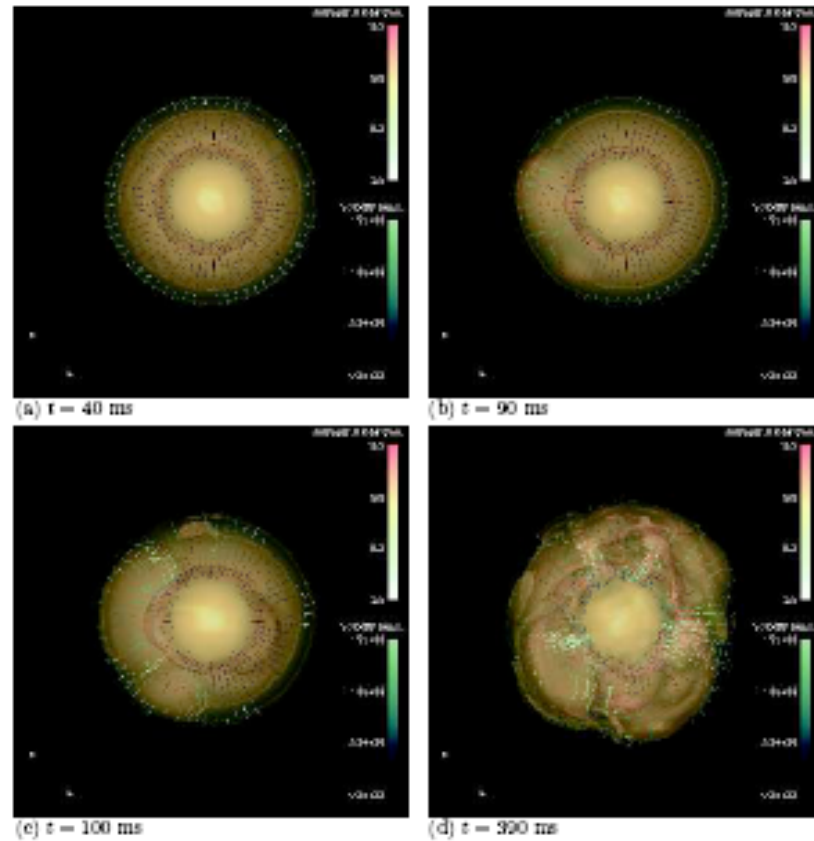Fig. 7.— The iso-entropy surfaces and velocity vectors in the meridian section for Model IV. The hemispheres $(0 \leq \phi \leq \pi)$ of eight iso-entropy surfaces are superimposed on one another with the outermost surface nearly corresponding to the shock front.
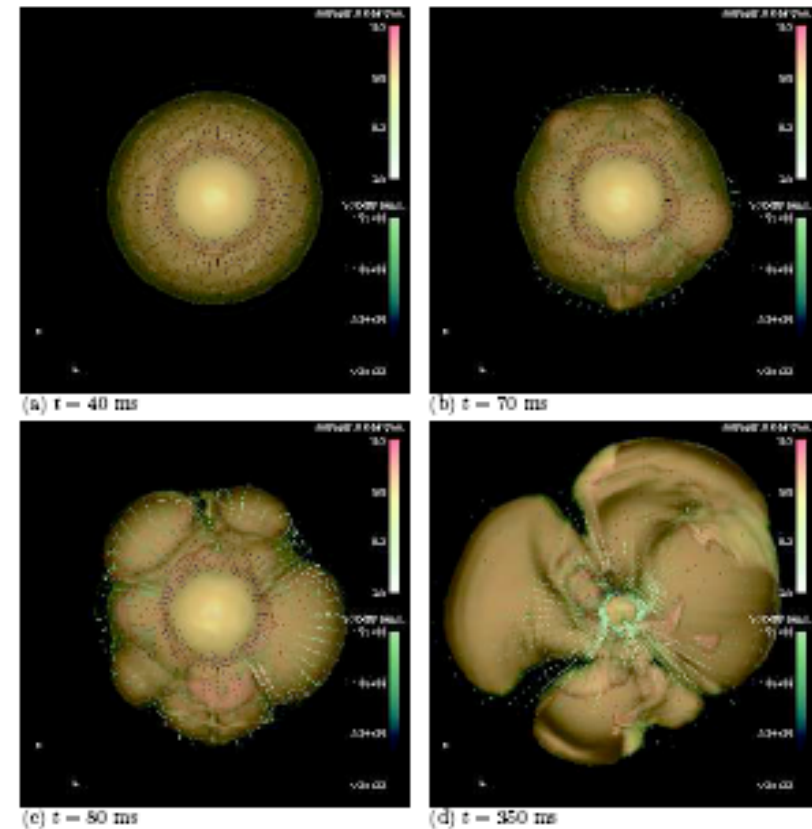
Fig. 8.— The iso-entropy surfaces and velocity vectors in the meridian section for the explosion model (Model VI). Note that the displayed region is 2.5 times larger for panel (d).

Iwakami etal. 2007 (3D)

Hydro-Magnetic Simulations
Livne etal,ApJS, 170,187,07; Burrows etal. ApJ,664,416,07, Dessart etal. ApJ,669,585; arXiv:0710.5789

First suggested by − Le-Blanc & Wilson 1970

The amplified magnetic stress on collapse
 injects rotational energy into bipolar jets, which,
 depending on the available energy, could trigger
 explosion.

 Here : 1st with realistic EOS and neutrino physics

Amplification of the magnetic field

1. Compression during collapse
2. Field winding due to rotation after bounce
3. MRI – the magneto-rotational instability on longer time scales

Magnetorotational Instability
(Balbus & Hawley 1991)

Magnetorotational Instability

- Stability requirement is

$$(k \cdot v_A)^2 > -\frac{d\Omega^2}{d \ln R}$$

- One can always find a small enough wavenumber k so there will be an instability unless

$$\frac{d\Omega^2}{d \ln R} > 0$$

MRI maximum growth

- Maximum unstable growth rate:

$$|\omega_{max}| = \frac{1}{2}\left|\frac{d\Omega}{d \ln R}\right|$$

- Maximum rate occurs for wavenumbers

$$(k \cdot v_A)^2_{max} = -\left(\frac{1}{4} + \frac{\kappa^2}{16\Omega^2}\right)\frac{d\Omega^2}{d \ln R}$$

- For Keplerian profiles maximum growth rate and wavelengths:

$$|\omega_{max}| = \frac{3}{4}\Omega$$

$$(k \cdot v_A)_{max} = \frac{\sqrt{15}}{4}\Omega$$

parametric input and results

TABLE 1

PROPERTIES OF MODELS

Name	Mass $(M_\odot)$	$B_{poloidal}$ (G)	Field Geometry	P_0 (s)	A_0 (km)	$\Delta\theta$ (deg)	$t_{explosion}$ (ms)	t_{end} (ms)	v_{max} (km s^{-1})	$E_{explosion}$ (10^{51} ergs)	Power (10^{51} ergs s^{-1})	$\langle P \rangle$ (ms)
M15B0DP2A1H	15	0	...	2	1000	90	...	595	...	...	...	3.70
M15B10DP2A1H	15	10^{10}	Dipole	2	1000	90	550	944	37000	0.03	0.155	3.14
M15B10DP2A1F	15	10^{10}	Dipole	2	1000	180	550	685	37000	0.03	0.118	3.18
M15B11DP2A1H	15	10^{11}	Dipole	2	1000	90	250	636	50000	0.2	0.661	6.17
M15B11UP2A1H	15	10^{11}	Uniform	2	1000	90	180	585	55000	2.0	6.832	3.98
M15B11DP4A1H	15	10^{11}	Dipole	4	1000	90	170	415	33000	0.005	0.050	4.21
M15B12DP2A1H	15	10^{12}	Dipole	2	1000	90	80	111	36000	0.6	3.168	25.60

MHD collapse – 36 M_o

Streamlines

M15B11UP2A1H
Velocity Streamlines
Time = 175.5 ms
Radius = 3500.00 km
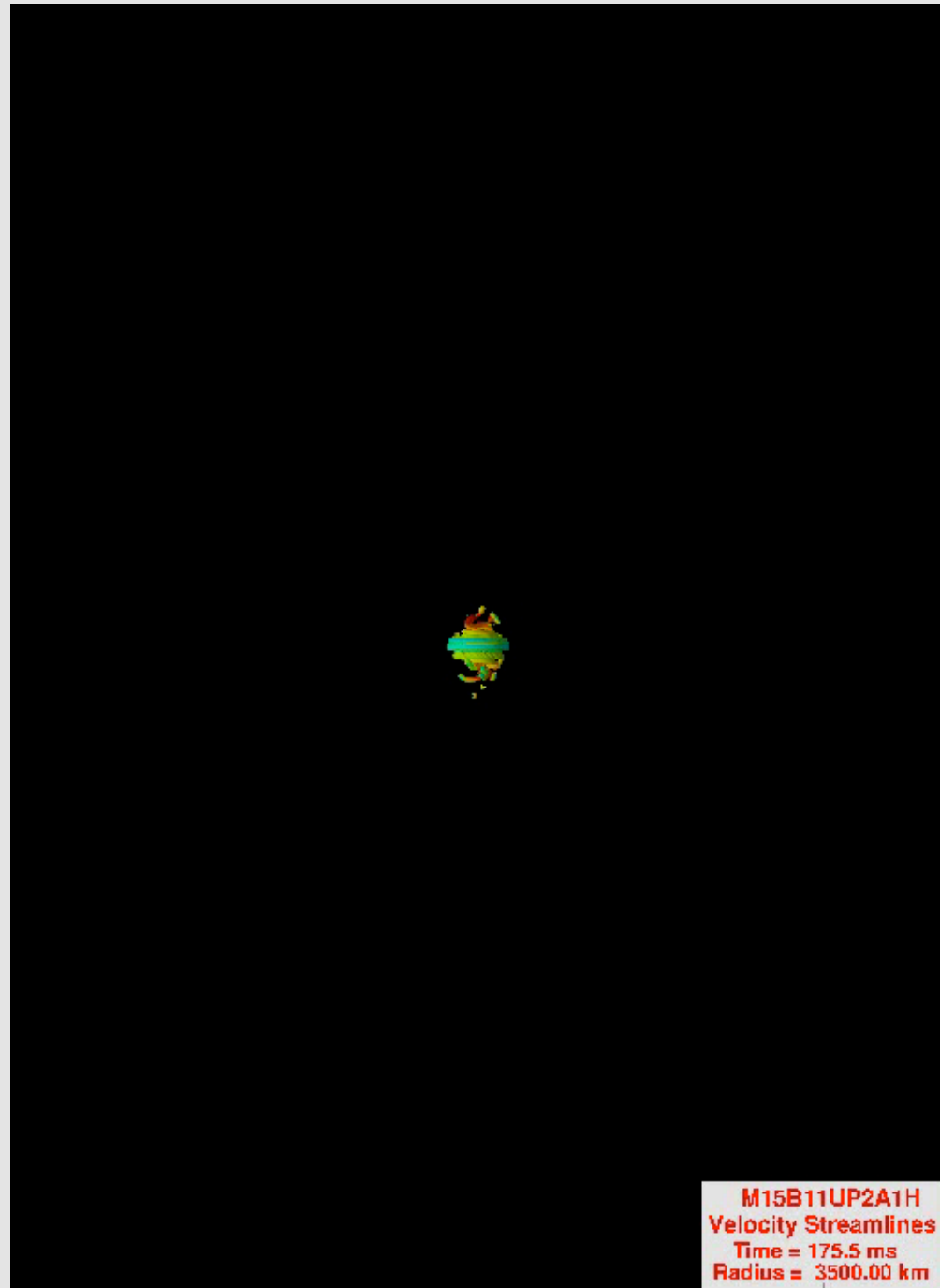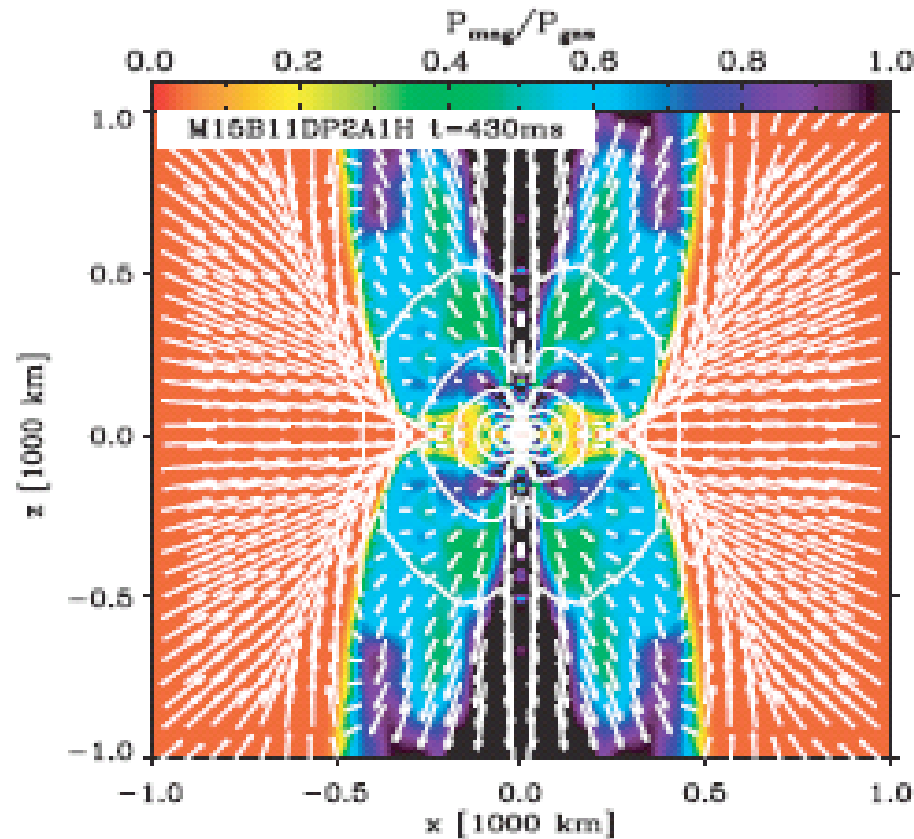
Hydro-magnetic flow structure

Fig. 9.— Color map for model M15B11DP2A1H at 430 ms after bounce of the ratio of magnetic to gas pressure, overplotted with white isodensity contours (every decade downward from 10^{14} g cm^{-3}) and velocity vectors (lengths saturated to 15% of the width of the figure and corresponding to a velocity of 10,000 km s^{-1}).

4. Lessons

A – SASI dominated collapse

1. Simulations should be carried for a long time (more than 1 second)

2. After 200 ms or so simulations with slightly different numerical parameters start to diverge.

3. Convection inside the PNS is not effective. Multipols expansion of gravity is not accurate enough – the missing short waves tends to over produce "convective" noise especially inside and around the core.

4. Finite difference grid solver, a la Shu, gives excellent conservation of linear momentum. However conservation of gravitational energy is still not satisfying.

5. Rapid rotation suppresses the SASI and the subsequent acoustic mechanism by reducing equatorial accretion.

Anisotropy of the radiation field (Ott etal. Astro-ph 2008arXiv0804.0239O)
Application of SN transport for rotating core of 20 M$_o$

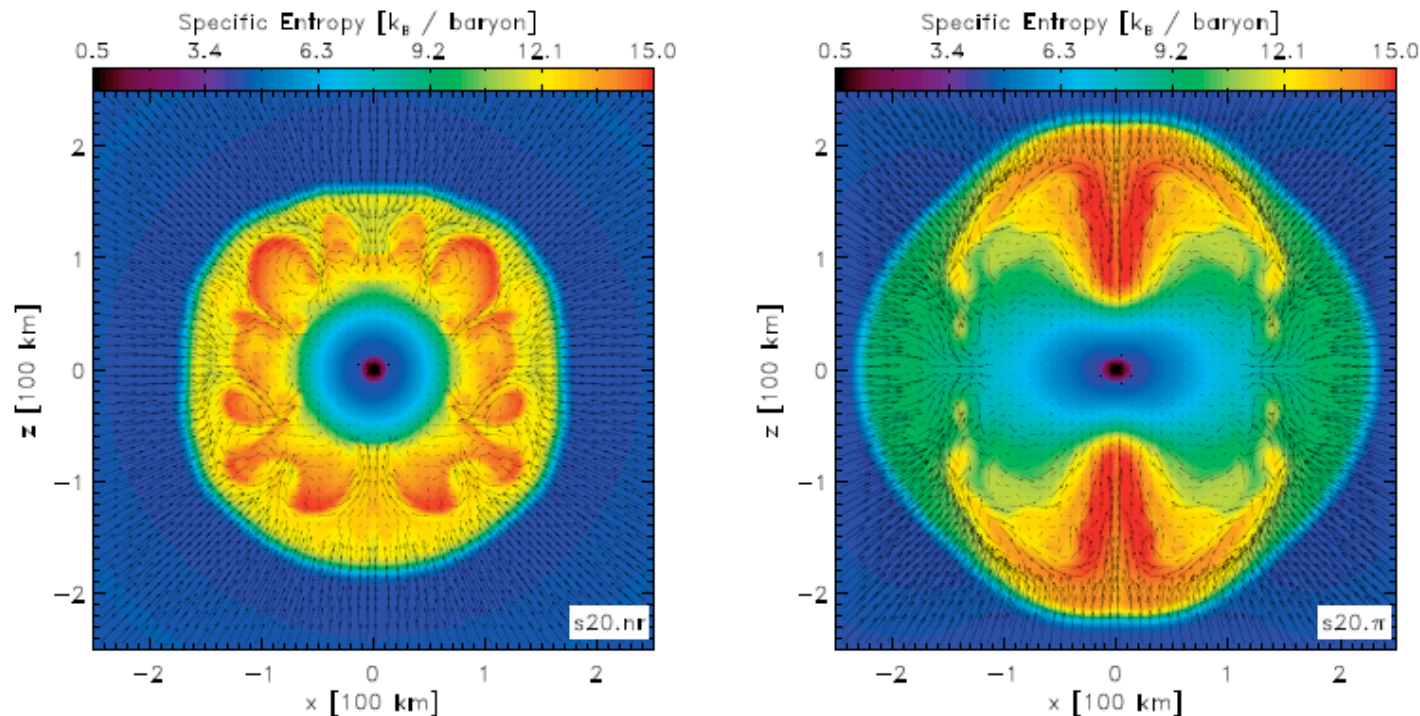- Rotation strongly affects convection and the SASI

FIG. 2.— Entropy colormaps of the nonrotating model s20.nr and the rotating model s20.π at 160 ms into their postbounce evolution computed with MGFLD. Velocity vectors are superposed with vector lengths saturated at 1.0×10^9 cm s^{-1}. Model s20.nr has a practically spherical PNS and shows features of violent overturn in the convectively unstable postshock region. The shock radius in this model is $\sim$175 km at this point and the onset of the SASI is apparent from the slightly deformed shock. Model s20.π, on the other hand, has a strongly rotationally-flattened PNS and convective overturn is confined to regions of low latitude. These regions exhibit the globally highest entropies and greatest entropy gradients, since the polar velocity divergence at the shock is the highest. The shock radius at this time in model s20.π is $\sim$230 km and no SASI features are visible.

continue

6. Transport simulations give very modest changes compared to FLMGD ones. Larger, but not dramatic, differences are seen in rotating models.

7. Rotation did not reveal any dramatic axial effects.

8. Core oscillations are seen very late, and therefore their amplitudes and power needs further investigation.

9. Yet, interesting shock interactions between the core and down stream funnels are seen in all simulations.

10. SASI amplitudes, and the entropy of the pre-shocked matter behind the main accretion shock, continuously grow due to successive secondary shocks. These shocks are generated by convective funnels bouncing off the core, and by colliding eddies. The role of secondary shocks in amplifying the SASI and possibly exciting core oscillations needs further investigation.

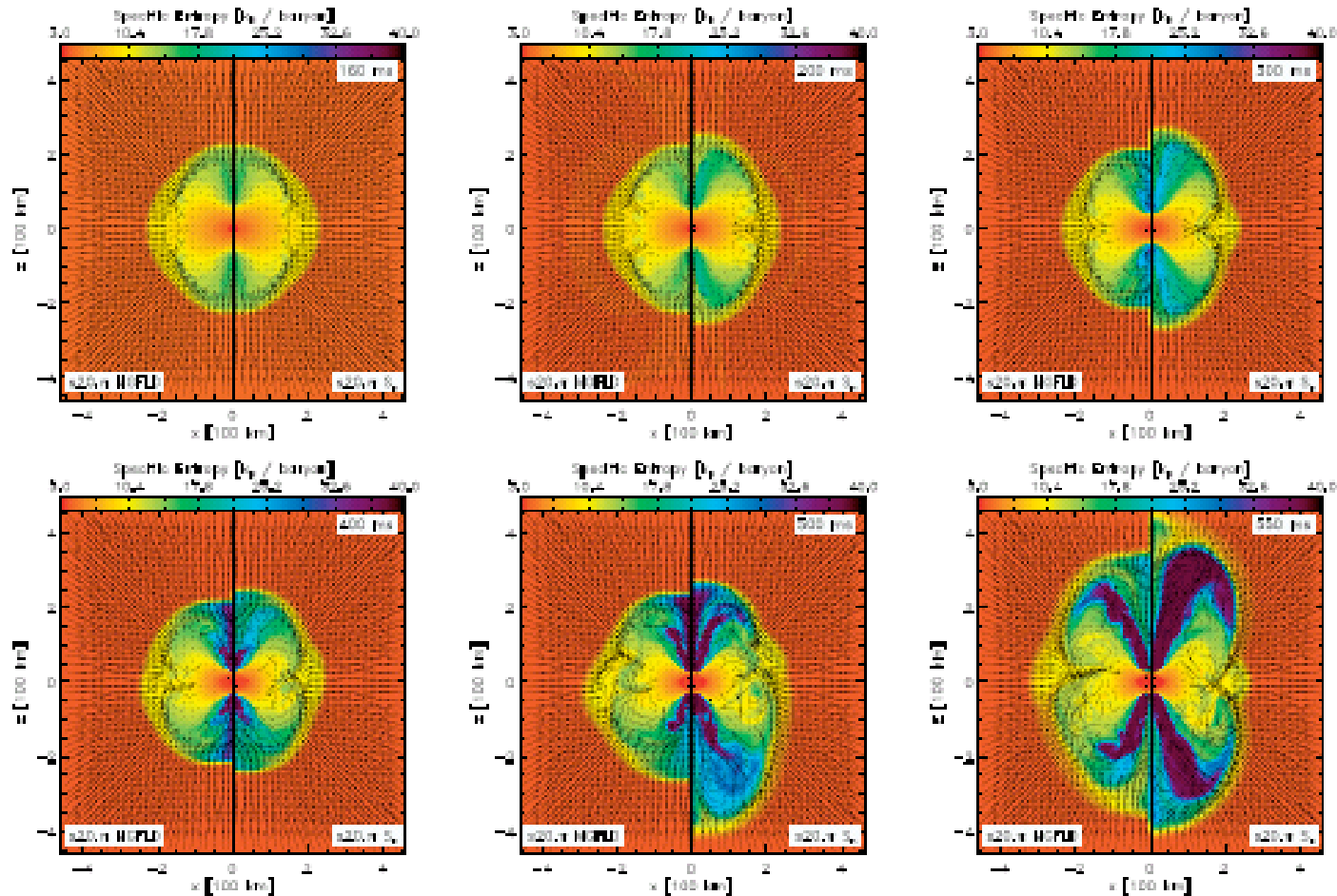# Neutrino Transport vs. Multi-group Diffusion

Fig. 21.— 2D entropy colormaps portraying the postbounce evolution of the rapidly-rotating model s20.π between 160 ms (top-left panel) and 550 ms (bottom-right panel) after core bounce. Fluid-velocity vectors are superposed to relay an impression of the flow and convey the partial suppression of convective overturn in regions of positive specific angular momentum gradient. As in Fig. 20, we plot the MGFLD result on the left-hand side and the S_n result on the right-hand side of each panel. Easily discernible is the immediate increase in the polar shock radius in the S_n calculation. This is a direct consequence of the increased polar neutrino heating in this variant (Figs. 15 and 16). At intermediate times, S_n and MGFLD shock positions grow closer, but later on in the postbounce evolution, the S_n variant begins to develop larger top-bottom SASI-like asymmetry and polar shock excursions at earlier time than its MGFLD counterpart.

Secondary shocks drive SASI
and increase the entropy of the pre-shocked matter
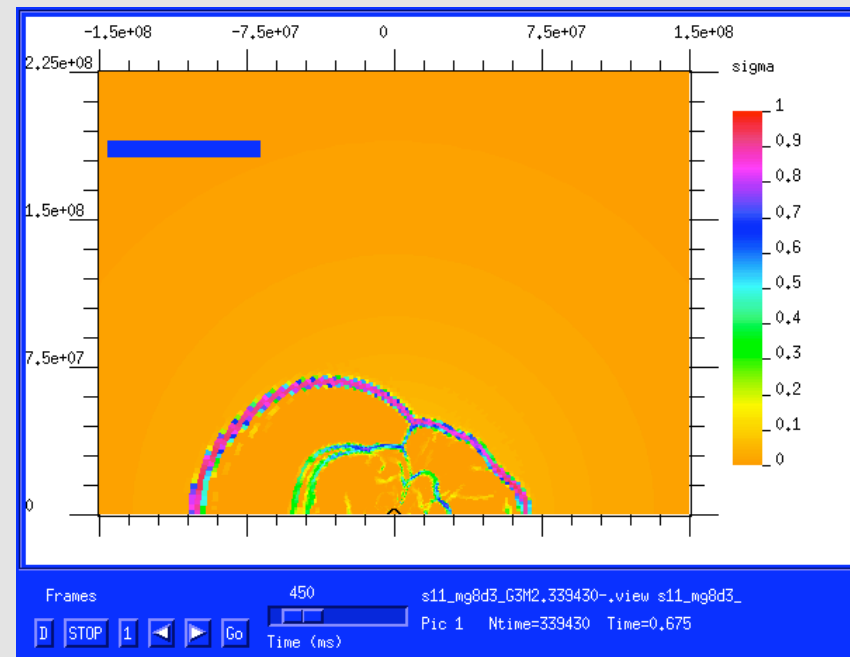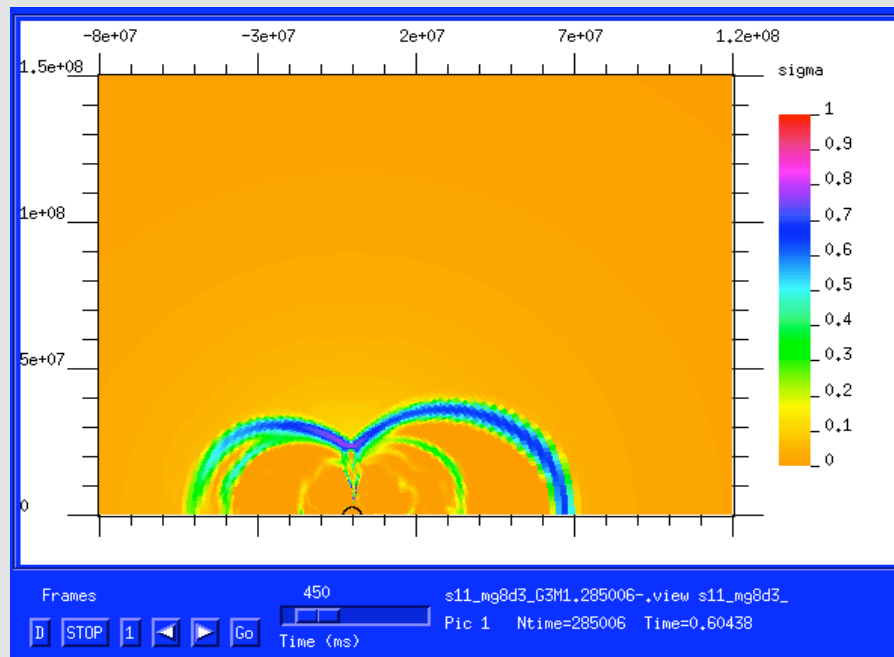
continue

11. In those cases where explosion is observed :

the energy budget is not clearly explained and the final (estimated) explosion energy is very uncertain.

B – MHD dominated collapse

1. **Fast initial rotation** (p= 2 sec) with **moderate initial B-field** ($Bz=10^{11}$ Gauss) lead to MHD dominated explosion with strong bipolar jets.

2. With lower initial rotation MHD driven currents can help explosion by other mechanisms, like neutrinos, and **imprint bipolar structures on the remnant.**

3. **Formation of strong jets is a stiff function of $Omega_o$.**

4. The mapping of the initial rotation to explosion energy is at large clear (**with uncertainties at the magnetic part**)

5. **MRI amplification was not captured** in the simulations due to too coarse mesh.

6. MHD effects can inhibit the formation of BH following the collapse of massive stars around 35 M_o !!

5. Conclusions and Future work

- The current code is reasonably accurate until roughly 300 ms, producing nice SASI type flow. For longer times we need to (and will) upgrade the current schemes, in particular the gravity solver, to higher order of accuracy.

- Improvements in the transport schemes (moments app.) will be introduced, but are not expected to change the general outcomes for neutrino-driven mechanism (with the current microphysics).

- Core oscillations and other mechanisms for generating secondary shocks need further investigations using the improved schemes. The efficiency of these shocks in converting accretion energy to heat is important.

- We confirm the LeBlanc-Wilson mechanism for MHD driven explosions with up-to-date neutrino physics, modest initial B and fast initial rotation.

Open questions and uncertainties

- Microphysics – EOS and neutrino cross-sections
- 3D effects
- Initial conditions for rotation and B fields.
- Small scales processes (turbulence, MRI)
- Nuclear burning at outer layers
- Mapping of progenitor parameters to explosions
- GR effects : important for massive progenitors and BH formation
- NS kicks, infall, r-processes : all need the extension of the simulations to a few seconds
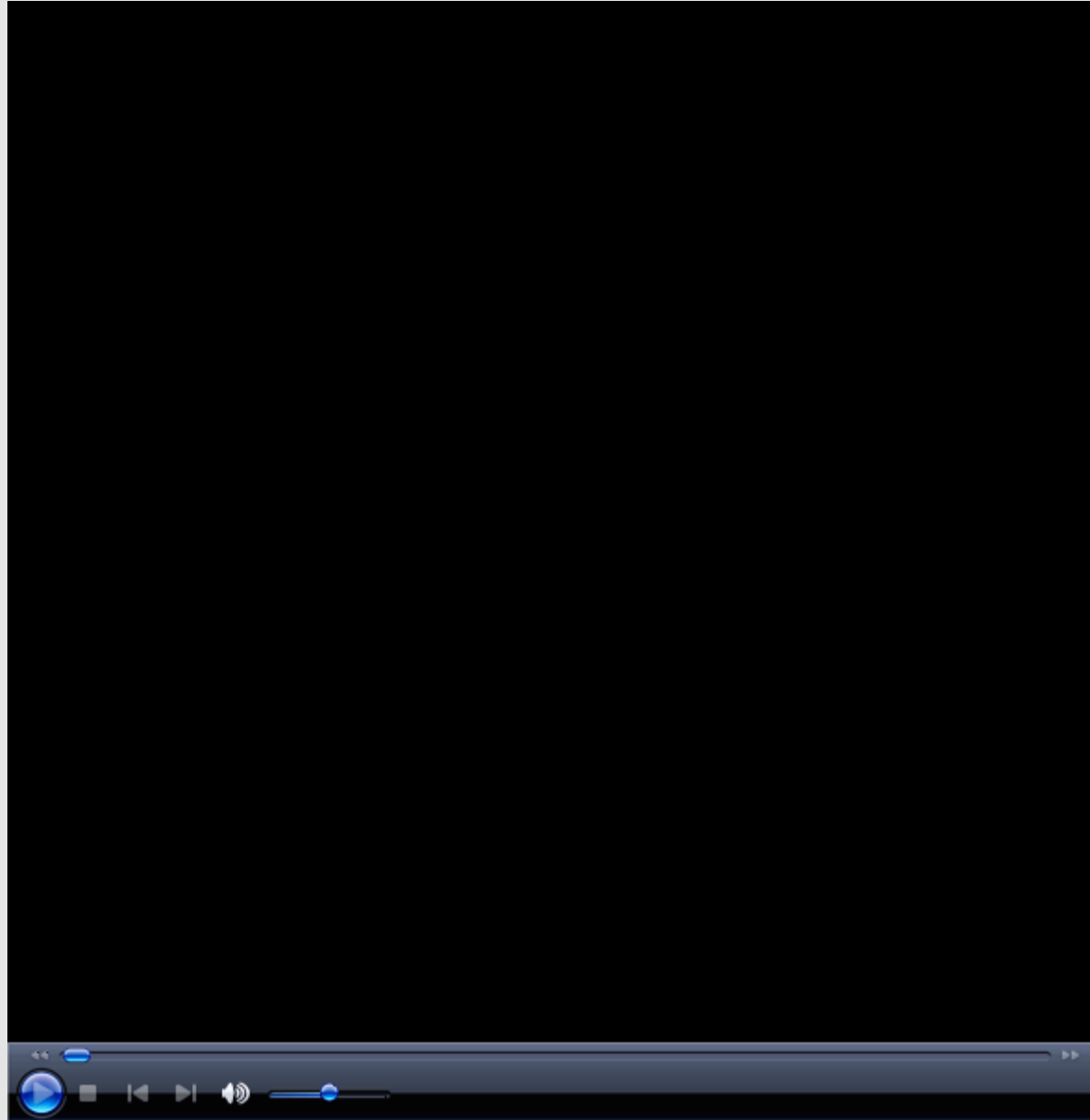
The "speculative" acoustic mechanism
(Burrows etal. ApJ 640,878, 2006)

- Strong SASI motions can excite non-radial core oscillations
- The strongest modes are L1 g-modes of high frequency
- The amplitudes of the oscillations grow as long as accretion and turbulent motion continue due to non-linear coupling
- The emitted acoustic waves deposit energy in the mantle more efficiently than the radiation field after 300-500 ms
- Very asymmetric explosions eventually obtained

The Problems :

- It is unique to V2D : at the moment no other code can verify this because of the central singularity
- May be a result of some yet unknown numerical artifact

Late Core Oscillations (11 M_o)

Analytic non-radial L1 mode

Acoustic explosion (11 M_o)

Another look (11 M$_o$)

Collapse of 20 M$_o$

Features of The Acoustic Mechanism

- Delayed onset of Advective-Acoustic/SASI Instability (200 ms)
- Nested/multiple shock waves; Entropy grows due to cycles of shocking and neutrino heating: Sets the Stage, but SASI not the agency of explosion
- Core l=1 g-modes are excited by turbulence and funnel accretion after 300 ms and persists
- Core Oscillation radiates acoustic power at high efficiency
- Acoustic radiation by core oscillation deposited in matter exceeds neutrino heating after ~350-400 ms
- Excitation by funnel accretion continues as long as it is needed to explode mantle - A natural means by which the supernova explosion is self-regulating !!
- Sound pulses steepen into multiple, nested shock waves; r-process entropies possible !!
- Unipolar explosion ("early"): simultaneous explosion and accretion; symmetry breaking (kick ?)
- Much left to do, verify, falsify, and test (!)

The Main Magnetic Effects

- Accretion through the stalled shock maintains strong B-field as long as it exists.
- Fast initial rotation (p= 2 sec) with moderate initial B-field ($Bz=10^{11}$ Gauss) lead to MHD dominated explosion with strong bipolar jets.
- With lower initial rotation MHD driven currents can help explosion by other mechanisms, like neutrinos.
- Formation of strong jets is a stiff function of $Omega_o$.
- Rapid rotation suppresses the SASI and the subsequent acoustic mechanism by reducing equatorial accretion.
- MRI amplification was not captured in the simulations due to too coarse mesh.
- MHD effects can inhibit the formation of BH following the collapse of massive stars around 35 M_o !!

The Limitations of Current Numerical Simulations

- The physical variables vary by many order of magnitude, imposing severe accuracy requirements on the numerical schemes !.
- Numerical dissipations are too strong
- The physical time (1s) covers many dynamical times
- About 1 million time steps (accumulation of numerical errors)
- The singularity of the center – damps L1 g-modes (except in V2D type codes)
- All multi-D schemes do not conserve energy and linear momentum exactly
- Full multi-group multi-angle transport of neutrinos is still too expensive, even in 2D

Current understanding of core-collapse

- Multi-D instabilities, mainly SASI, can help neutrino-driven explosions, probably at low masses.

- Strong enough SASI, can excite core oscillations that eventually lead to explosion by depositing enough acoustic energy into the envelop.

- MHD-driven explosions need high initial rotation, and then other instabilities are not important. With lower initial rotation MHD explosions do not occur, but still, important jet features are present (bipolar structures of the ejecta) which can help other mechanisms.

- MHD effects may inhibit the formation of black holes during the collapse of massive stars ($M_o > 35$). Implications for the collapsar model of long duration GRB's are under investigation.

- The present numerical tools can not give quantitative answers to many of those issues and many subjects are debated.